JOURNAL OF THERMOPHYSICS AND HEAT TRANSFER
Vol. 29, No. 1, January–March 2015

Natural Convection from Vertical Parallel Plates: An Integral Method Solution

Mehran Ahmadi,* Mohammad Fakoor-Pakdaman,* and Majid Bahrami†
Simon Fraser University, Surrey, British Columbia V3T 0A3, Canada

DOI: 10.2514/1.T4308

Steady-state external natural convection heat transfer from isothermal, vertically mounted rectangular fins is modeled analytically. An integral technique is used to solve the governing equations. Compact relationships are developed for the velocity and temperature profiles for the buoyancy-driven channel flow for the $1000 \leq Ra_s \leq 4500$ range. Comprehensive numerical and experimental studies are performed. The proposed analytical model is successfully validated against the numerical data with the maximum relative differences of 9.8 and 3.5% for velocity and temperature profiles, respectively. Also, new semianalytical local and average Nusselt numbers are reported as functions of the Rayleigh number, temperature difference, and fin aspect ratio; and they are compared against the experimental data with good accuracy of 1.6% maximum relative difference.

Nomenclature

c_p	=	specific heat, J/kg · K
$\dot{E}$	=	energy, W
F	=	force, N
Gr	=	Grashof number; $g\beta\Delta Ts^3/\nu^2$
g	=	gravitational acceleration, m/s^2
H	=	fin height (length in z direction), m
h	=	convection heat transfer coefficient, W/m^2 K
k	=	thermal conductivity, W/mK
L	=	base plate length, m
l	=	fin length, m
$\dot{M}$	=	momentum, (kg · m)/s
m	=	mass, kg
$\dot{m}$	=	mass flow rate, kg/s
Nu	=	Nusselt number; hs/k
P	=	electrical power, W
Pr	=	Prandtl number; ν/α
q	=	heat flux per unit depth in z direction, W/m
Q	=	heat transfer rate, W
Ra	=	Rayleigh number; $g\beta\Delta Ts^3/\nu\alpha$
T	=	temperature, K
t	=	fin thickness, m
U	=	nondimensional velocity; us/α
u	=	flow velocity in y direction, m/s
W	=	base plate width, m
X	=	nondimensional x, x/l
x	=	direction parallel to fin surface, m
Y	=	nondimensional y; y/s
y	=	direction normal to fin surface, m
z	=	direction normal to x and y in Cartesian coordinate
α	=	thermal diffusivity, m^2/s
β	=	coefficient of volume expansion, 1/K
ΔT	=	temperature difference; $T_w - T_\infty$
ε	=	aspect ratio of the channel; l/s
θ	=	nondimensional temperature; $T_w - T/T_w - T_\infty$
μ	=	fluid dynamic viscosity, (N · s)/m^2
ρ	=	density, kg/m^3
τ	=	shear stress per unit depth in z direction, N/m

Subscripts

C.V.	=	control volume
F.D.	=	fully developed
N.C.	=	natural convection
Rad.	=	radiation
w	=	wall properties
∞	=	ambient properties

Received 23 October 2013; revision received 29 April 2014; accepted for publication 27 July 2014; published online 3 November 2014.

*Laboratory for Alternative Energy Conversion, Mechatronic Systems Engineering, No. 4300, 250-13450 102nd Avenue.

†Laboratory for Alternative Energy Conversion, Mechatronic Systems Engineering, No. 4300, 250-13450 102nd Avenue; mbahrami@sfu.ca (Corresponding Author).

I. Introduction

EFFICIENT thermal management of electronics, such as power-electronics, light-emitting diodes (LEDs), and telecommunication devices, is essential for optimum performance and durability. The rate of failures due to overheating nearly doubles with every 10°C increase above the operating temperature [1]. Considering the increasing functionality and performance of electronic devices and the ever increasing desire in miniaturization in the industry, thermal management has become the limiting factor in the development of such devices (e.g., power electronics [2,3], telecommunications [4], and LEDs [5,6]), and reliable and low-cost methods of cooling are required more and more. Consequently, electronics thermal management is of crucial importance, as is reflected in the market. The thermal management technologies market was valued at $6.7 billion in 2011 and reached $7 billion in 2012. The total market value is expected to reach $10.1 billion in 2017 after increasing at a five year compound annual growth rate of 7.6%. Thermal management hardware, e.g., fans and heatsinks, accounts for about 84% of the total market. Other cooling product segments, e.g., software, thermal interface materials, and substrates, each account for between 4 to 6% of the market [7].

Telecommunication devices are examples of electronic systems that require efficient thermal management. More than 1% of global total energy consumption, and 3% of U.S. energy consumption, in 2012 was used by telecommunication devices [8]. This is equal to energy consumed by 15 million U.S. homes, with an equivalent CO2 emission of 29 million cars [9,10]. This value is predicted to increase by 50% by 2017 [11]. About 28% of this energy is required for cooling and thermal management of such systems [12].

Passive cooling is a widely preferred cooling method for electronic and power electronic devices, since it is an economical, quiet, and a reliable method. Moreover, natural convection, and other passive cooling solutions, require no parasitic power, which make them more attractive for sustainable and "green" systems. Integrating passive cooling techniques with conventional cooling strategies in the telecommunication industry can reduce the energy required for thermal management from 28% of current total energy consumption to 15% [13] in general, and 0% [14] in some cases. As such, passive cooling

systems have attracted immense attention, especially in the renewable energy conversion systems and applications in which efficiency is of major importance or applications where using a fan is not essential or is impossible, e.g., hostile environments (contaminated air, vibrations, noise, or humidity).

Finned surfaces are widely used for the enhancement of heat transfer [15,16]. Natural convective heat transfer form vertical rectangular fins is a well-established subject in the literature. Pioneering analytical work in this area was carried out by Elenbaas [17]. He investigated the isotheral finned heatsink semianalytically and experimentally. His study resulted in general relations for an average Nusselt number for vertical rectangular fins, which was not accurate for small values of fin spacing. Churchill [18] and Churchill and Chu [19] developed a general correlation for the average Nusselt number for vertical channels using the theoretical and experimental results reported by a number of authors. Bar-Cohen and Rohsenow [20] also performed a semianalytical study to investigate the natural convective heat transfer from two vertical parallel plates. They developed a relationship for the average Nusselt number as a function of the Rayleigh number for isothermal and isoflux plates. Bodoia and Osterle [21] followed Elenbaas [17] and used a numerical approach to investigate the developing flow in a vertical and the natural convection heat transfer between symmetrically heated, isothermal plates in an effort to predict the channel length required to achieve fully developed flow as a function of the channel width and wall temperature. Ofi and Hetherington [22] used a finite element method to study the natural convective heat transfer from open vertical channels. Culham et al. [23] also developed a numerical code to simulate the free convective heat transfer from a vertical fin array. Several experimental studies were carried out on this topic. Sparrow and Acharya [24], Starner and McManus [25], Welling and Wooldridge [26], Edward [27], Chaddock [28], Aihara [29–32], Leung and Probert [33], Leung et al. [34–36], Leung and Probert [37–39], and Van de Pol and Tierney [40] are some examples. These studies were mostly focused on the effects of varying fin geometric parameters, the array, and base plate orientation. Table 1 provides a brief overview on the pertinent literature; more detailed reviews can be found elsewhere, e.g., [41].

All the aforementioned studies reported average Nusselt numbers for natural convective heat transfer from vertical rectangular fins; however, to the best knowledge of the authors, velocity profile, temperature profile, and the local Nusselt number for the channel are not available in the literature. It should be mentioned that the velocity profile has been reported for the special case of fully developed flow in a very long channel [42]. An in-depth understanding of the velocity and temperature profiles is needed for the development of next-generation efficient cooling solutions. Complexities such as chimney effect, coupled governing equations, etc., cause the finding of full analytical solutions for the temperature and velocity domain to be highly unlikely. As such, in this study, an integral technique is used to present closed-form solutions for the velocity and temperature distributions in laminar natural convection inside a vertical channel made by two neighboring fins.

II. Problem Statement

The main objective of this study is to develop a compact, analytical model that can predict the natural convective heat transfer from a squared array of vertically mounted, rectangular isothermal fins (see Fig. 1). Figure 1c schematically shows the front view of the considered geometry for two fins in the fin array. Due to symmetry, only one channel can represent the entire fin array.

The assumptions used in this study are listed as follows: 1) steady-state two-dimensional heat transfer and fluid flow (fins are assumed long enough in the direction normal to the surface); 2) isothermal fins, at T_w; 3) constant thermophysical properties, except for the fluid density; and 4) Boussinesq approximation for change of density as a function of temperature [42].

It is assumed that the fin height in the z direction is large enough that the effects of the base plate can be neglected and the problem can be treated as a two-dimensional flow.

An integral technique is used to solve the governing equations subjected to constant wall temperature boundary conditions. The integral technique is a powerful analysis developed by Pohlhausen and von Kármán in the first decade of 20th century to obtain approximate solutions to complex problems [42]. It works based on the principal that the general behaviors of the velocity and temperature profiles are known. Assuming a profile for each, and satisfying conservation of mass, momentum, and energy in a lumped fashion across the region of interest, we can obtain velocity and temperature profiles within an acceptable accuracy by satisfying the boundary conditions. The conservation laws can be written for the control volume shown in Fig. 1c. Table 2 summarizes the integral form of the momentum and energy balance equations for the considered integral control volume. To find more details about the methodology to obtain the governing equations from the control volumes shown in Table 2, readers are invited to see the Appendix. The conservation equations are subjected to the following boundary conditions:

$$\text{At } y = 0; \qquad \frac{\partial u(x,0)}{\partial y} = \frac{\partial T(x,0)}{\partial y} = 0 \tag{1}$$

$$\text{At } y = s/2; \qquad u\left(x, \frac{s}{2}\right) = 0 \quad \text{and} \quad T\left(x, \frac{s}{2}\right) = T_w \tag{2}$$

Table 1 Summary of pertinent literature on natural convective heat transfer from a vertical rectangular fin

Reference	Method	Ra	Nu	Highlights
[28]	Empirical		$Nu_s = \frac{1}{24} Ra_s \left(\frac{s}{l}\right)\left\{1 - e^{-12.5/[Ra_s.(s/l)]^{3/4}}\right\}$	Isothermal
[19]	Analytical/empirical	All	$Nu_L = \left\{0.825 + \frac{0.387 Ra_l^{1/6}}{[1+(0.492/Pr)^{9/16}]^{8/27}}\right\}^2$	Isothermal isoflux
[27]	Empirical	10^4–10^9	$Nu_L = 0.59 Ra_l^{1/4}$	
[17]	Analytical/empirical	10^{-1}–10^5	$Nu_s = \frac{1}{24} Ra_s[1 - \exp[-\frac{35}{Ra_s}]]^{3/4}$	Symmetric isothermal
[20]	Analytical/empirical	All	$Nu_s = \left[\left(\frac{24}{Ra_s}\right)^2 + \left(\frac{1}{0.59 Ra_s^{0.25}}\right)^2\right]^{-0.5}$	Symmetric isothermal
			$Nu_s = \left[\left(\frac{6}{Ra_s}\right)^2 + \left(\frac{1}{0.59 Ra_s^{0.25}}\right)^2\right]^{-0.5}$	Asymmetric isothermal
[28]	Empirical/numerical		$Nu_s = \left[\left(\frac{12}{(s/L)Ra_s}\right)^2 + \left(\frac{1}{0.619((s/L)Ra_s)^{0.25}}\right)^2\right]^{-0.5}$	Isothermal
[24]	Empirical	$s < 50$ mm	$Nu_s = 6.7 \times 10^{-4} Ra_s\left[1 - \exp\left(\frac{7460}{Ra_s}\right)^{0.44}\right]^{1.7}$	Isothermal horizontal
		$s > 50$ mm	$Nu_s = 0.54 Ra_s^{0.25}$	
[39]	Empirical	$Ra < 10^6$	$Nu_s = 0.135 Ra_s^{0.5}$ $Ra < 250$ $Nu_s = 0.423 Ra_s^{0.333}$ $250 < Ra < 10^6$	Small fin heights
	Empirical	$Ra < 10^6$	$Nu_s = 0.144 Ra_s^{0.5}$ $Ra < 250$ $Nu_s = 0.490 Ra_s^{0.333}$ $250 < Ra < 10^6$	

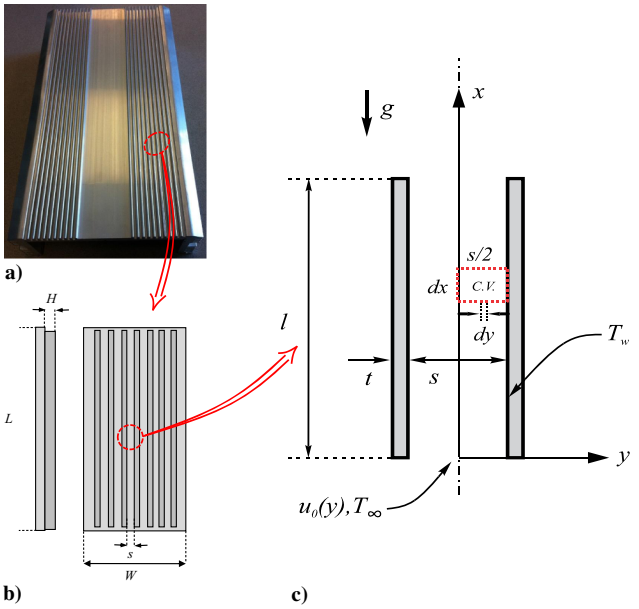

Fig. 1 Representations of a) naturally cooled enclosure of a dc–dc converter; b) schematic of the heat sink; and c) solution domain, selected as the control volume representing the heat sink.

$$\text{At } x = 0 \qquad u(0, y) = u_0(y) \quad \text{and} \quad T(0, y) = T_\infty \tag{3}$$

$$\text{As } x \to \infty \qquad u(x \to \infty, y) = u_{\text{F.D.}}(y) \quad \text{and} \quad T(x \to \infty, y) = T_w \tag{4}$$

Equation (1) is concluded from the symmetry at the centerline of the channel. The parameter $u_0(y)$ represents the velocity profile at the channel inlet and will be discussed later in Sec. III.A. It should be noted that the velocity at the channel inlet cannot be zero, since the velocity has a nonzero profile at the channel outlet and conservation of mass implies that the velocity should have a nonzero profile in the inlet.

III. Present Solution

The first step, before solving the governing equations, is to determine the velocity profile at the inlet of the channel; $x = 0$ [Eq. (1)]. The following section presents the details on how $u_0(y)$ can be obtained.

A. Entrance Velocity

To find the velocity profile at $x = 0$, conservation of mass can be written for a control volume enclosing the entire domain between the fins, as shown in Eq. (5). We assumed the channel is long enough so that, at the outlet, velocity reaches its fully developed profile and the fluid temperature will be equal to the wall temperature. Since the cross-section area is constant and fluid enters the channel with the ambient temperature, mass balance can be written as

$$\rho|_{T=T_w} u_{\text{F.D.}}(y) = \rho_\infty u_0(y) \tag{5}$$

Knowing the fully developed, velocity profile at the outlet of parallel fins from [42],

$$u_{\text{F.D.}}(y) = \frac{g\beta\Delta T s^2}{8\nu}\left(1 - \frac{4y^2}{s^2}\right) \tag{6}$$

Equation (5) is the conservation of mass between the inlet and the outlet of the channel. To find the density at the outlet that is assumed to be at the wall temperature, Boussinesq approximation is used:

$$\rho(T) = \rho_\infty[1 - \beta(T - T_\infty)] \tag{7}$$

Substituting T_w for T in Eq. (7) and substituting the result in Eq. (5), $u_0(y)$ can be found as

Table 2 Integral form of conservation equations for the integral control volume[a]

Equation	Schematic of C.V.	Terms description	Conservation equation
Momentum	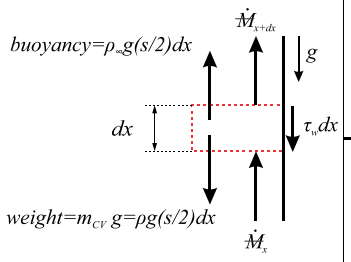	$\dot{M}_x = 2\rho\int_0^{s/2} u^2(x,y)dy$ $\dot{M}_{(x+dx)} = 2\rho\int_0^{s/2} u^2(x,y)dy$ $+\frac{\partial}{\partial x}(2\rho\int_0^{s/2} u^2(x,y)dy)$	$\frac{\partial}{\partial x}\int_0^{s/2} u^2(x,y)dy + \frac{\tau_w}{\rho}$ = $g\beta\int_0^{s/2}(T(x,y)-T_\infty)dy$
Energy	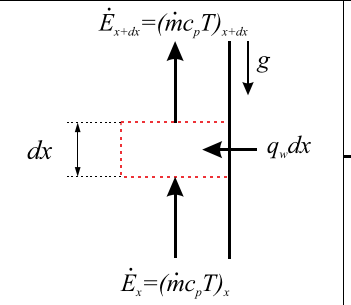	$\dot{E}_x = 2c_p\rho\int_0^{s/2} u(x,y)T(x,y)dy$ $\dot{E}_{(x+dx)} = 2c_p\rho\int_0^{s/2} u(x,y)T(x,y)dy$ $+\frac{\partial}{\partial x}(2c_p\rho\int_0^{s/2} u(x,y)T(x,y)dy)$	$\frac{\partial}{\partial x}\int_0^{s/2} u(x,y)T(x,y)dy$ = $\frac{q_w}{c_p}$

[a] Note that the buoyancy and weight forces are written for the unit depth.

$$u_0(y) = \frac{(1-\beta\Delta T)\Delta T g\beta s^2}{12\nu}\left(1-\frac{4y^2}{s^2}\right) \tag{8}$$

Now, all the boundary conditions are known, and an integral technique can be implemented to find the velocity and temperature profiles in the channel, as will be discussed in the following section.

B. Integral Technique

A second-order polynomial in the y direction is assumed for both the temperature and velocity profiles

$$u(x,y) = a_1(x)y^2 + b_1(x)y + c_1(x) \tag{9}$$

$$T(x,y) = a_2(x)y^2 + b_2(x)y + c_2(x) \tag{10}$$

Applying the boundary conditions in the y direction [Eqs. (1) and (2)] into Eqs. (9) and (10), we will have

$$u(x,y) = f(x)\left(y^2 - \frac{s^2}{4}\right) \tag{11}$$

$$T(x,y) = g(x)\left(y^2 - \frac{s^2}{4}\right) + T_w \tag{12}$$

Both $f(x)$ and $g(x)$ are unknown functions to be found, and they can be interpreted as the velocity and temperature at the centerline of the channel along the x direction. Physics of the flow and heat transfer suggest that both velocity and temperature at the centerline would increase rapidly at the beginning of the channel (developing region) and approach an asymptotic value as the fluid moves along the x axis (fully developed flow). Using the similarity solution technique for buoyancy-driven flow, Sparrow and Gregg [43,44] showed the temperature variation that gives rise to a similarity in the laminar boundary-layer governing equations is either a power law or exponential distributions. Similar assumptions have been made by Gebhart et al. [45] and Jaluria and Gebhart [46] for solving natural convection heat transfer equations in buoyancy-induced flow over an adiabatic vertical surface and laminar natural convection plume above a horizontal line heat source. Therefore, a general exponential behavior can be assumed for $f(x)$ and $g(x)$ as follows:

$$f(x) = -\frac{s^2}{4}(m - ne^{-px}) \tag{13}$$

$$g(x) = -\frac{s^2}{4}(\eta - \delta e^{-\gamma x} - T_w) \tag{14}$$

where m, n, p, η, δ, and γ are constants that should be determined. The coefficient $(-s^2)/4$ in Eqs. (13) and (14) and T_w in Eq. (14) are added for convenience and have no effect on the generality of the solution. Having Eq. (8), substituting Eqs. (13) and (14) into Eqs. (11) and (12), and applying the boundary conditions in the x direction, the parameters m, n, η, and δ will be determined as follows:

$$m = \frac{1}{8}\frac{g\beta\Delta T s^2}{\nu} \tag{15}$$

$$n = \frac{1}{8}\frac{g\beta^2\Delta T^2 s^2}{\nu} \tag{16}$$

$$\eta = T_w \tag{17}$$

$$\delta = \Delta T \tag{18}$$

Table 3 Nondimensional parameters

Parameter	Description
X	x/l
Y	y/s
U	us/α
θ	$(T_w - T)/(T_a - T_\infty)$
ε	l/s
Pr	ν/α
Gr_s	$g \cdot \beta \cdot \Delta T/\nu^2$
Ra_s	$Gr_s Pr$

Substituting the preceding calculated constants in Eqs. (11) and (12), and solving the integrated energy and momentum equations (Table 1), the two remaining constants, p and γ, can be obtained. After some mathematical manipulations, the velocity and temperature domain can be determined in the form of Eqs. (19) and (20):

$$u(x,y) = \frac{g\beta\Delta T}{4\nu}(\beta\Delta T e^{-(40\nu^2(3\beta\Delta T^2 - 4\Delta T)x/g\beta^2 s^4\Delta T^3(1-\beta\Delta T))} - 1) \times \left(y^2 - \frac{s^2}{4}\right) \tag{19}$$

$$T(x,y) = \frac{4\Delta T}{s^2} e^{-(120\alpha\nu x/g\beta\Delta T s^4(1-\beta\Delta T))}\left(y^2 - \frac{s^2}{4}\right) + T_w \tag{20}$$

Equations (19) and (20) can be presented in a more compact form, after nondimensionalizing, by introducing the dimensionless parameters shown in Table 3.

Using dimensionless parameters, the velocity and temperature distribution inside the channel can be presented as

$$U(X,Y) = -\frac{1}{4}Ra_s\left(1 - \beta\Delta T e^{-(160(1-(3/4)\beta\Delta T)/\beta\Delta T(1-\beta\Delta T))(\varepsilon X/Gr_s)}\right) \times \left(Y^2 - \frac{1}{4}\right) \tag{21}$$

$$\theta(X,Y) = 4\exp\left(-120\frac{\varepsilon X}{Ra_s(1-\beta\Delta T)}\right)\left(Y^2 - \frac{1}{4}\right) \tag{22}$$

IV. Numerical Study

To validate the present analytical model, an independent two-dimensional numerical model of the problem is developed in the commercially available software package ANSYS FLUENT 14.0. To couple the momentum and energy equations and add the buoyancy effects to the simulation, Boussinesq approximation is imposed to the air density behavior as a function of temperature, and gravity effect is added to the domain as body force in the negative y direction. Figure 2a shows a schematic of the domain considered for the numerical simulation, along with the boundary conditions assumed for the channel. The pressure inlet, $p = 1$ atm, and constant temperature, $T = T_\infty$, are applied at the bottom of the domain as the boundary condition. For the top of the domain, the pressure outlet boundary condition is applied, which imposes the pressure to be 1 atm. A no-slip isothermal solid surface ($u = 0$ and $T = T_w$) is considered for the channel wall, and the symmetry boundary condition is assumed for the centerline, which imposes no momentum and heat transfer, in the direction normal to the boundary. The parameters chosen for the benchmark case are shown in Table 4.

To ensure a mesh-independent solution, different grid sizes were tested and the total heat transfer rate from the fins was chosen as a monitoring parameter. Figure 3 shows the mesh-independency analysis for the benchmark case. For the mesh number of approx-

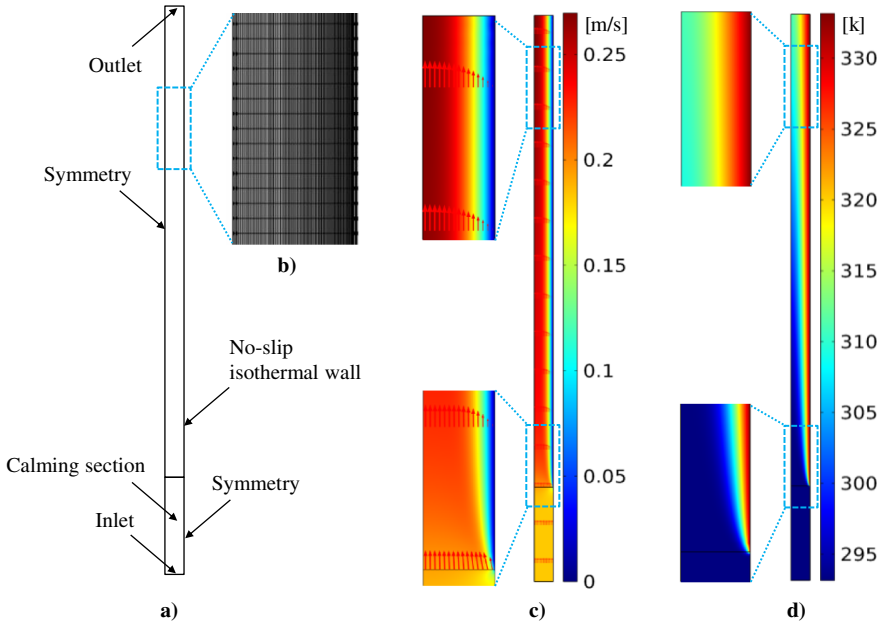

Fig. 2 Representations of a) numerical domain and boundary conditions, b) grid, c) velocity, and d) temperature domain for the benchmark case.

imately 900, we found that the simulation gives approximately 0.85% deviation in the average heat transfer rate from walls as compared to the simulation with a mesh number of 3000, whereas for the number of elements less than 900, the model does not converge to a reasonable solution. The relative deviations for the average wall heat flux are 0.20, 0.05, 0.02, 0.01, and 0.00% for 10,000, 20,000, 30,000, 40,000, and 50,000 number of elements, respectively. As a result, 40,000 elements are chosen for numerical simulations, as shown in Fig. 2b. The maximum skewness, calculated based on the equilateral volume method, is 0.21, which assured high quality of the grid. A finer mesh size is applied near the walls to resolve the boundary layer more accurately (see Fig. 2b). Samples of the velocity and temperature domains are shown as results of the numerical studies in Figs. 2c and 2d.

V. Experimental Study

A custom-made testbed was designed and built in order to validate the results from the integral solution and the numerical simulations. Five samples with variations in fin spacing were prepared, and a series of tests with different surface temperatures were conducted.

A. Testbed

A custom-made testbed was designed for measuring natural convection heat transfer from the finned heat sinks, as shown in Fig. 4. The setup included an enclosure made of polymethyl methacrylate (also known as Plexiglas), which is insulated by a layer of foam with a thickness of 15 mm. The testbed also included 20-cm-long 150 W Chromalox strip heaters, which were attached to the backside of the fins base plate, and a data acquisition (DAQ) system, supplied by National Instruments. High-conductive thermal paste provided by Omega was used to decrease the thermal contact resistance between the heater and the sample base plate. The voltage and the current of the supplied power were measured with an Agilent 34405A digital multimeter.

Table 4 Parameters used for the numerical simulation benchmark

Parameter	Description	Value	Unit
l	Wall length	10	cm
s	Wall spacing	8	mm
T_∞	Ambient temperature	20	°C
T_w	Wall temperature	60	°C
Ra_s	Rayleigh number	1.7×10^3	—

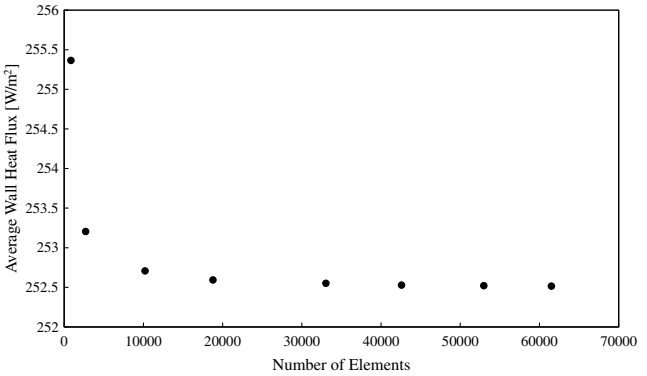

Fig. 3 Grid-independency study for the benchmark case (see Table 4).

Five samples with the same base plate size and different fin spacing and fin height, as shown in Table 5, were prepared.

B. Uncertainty Analysis

Voltage V and current I are the electrical parameters measured in our experiments, from which the input power P_{input} can be calculated. The total accuracy in the measurements is evaluated based on the accuracy of the employed instruments. The maximum uncertainty for the measurements can be obtained using the uncertainty concept provided in [47]. To calculate the uncertainty with the experimental measurements, the following relation is used [47]:

$$\omega_R = \left[\sum \left(\frac{\partial R}{\partial x_i}\omega_i\right)^2\right]^{1/2} \tag{23}$$

where ω_R is the uncertainty in results, $R(x_1, x_2, \ldots x_n)$; and ω_i is the uncertainty of the independent variable x_i. The final form of the uncertainty for the input power becomes

$$P_{\text{input}}[W] = VI \tag{24}$$

$$\frac{\delta P_{\text{input}}}{P_{\text{input}}} = \left[\left(\frac{\delta V}{V}\right)^2 + \left(\frac{\delta I}{I}\right)^2\right]^{1/2} \tag{25}$$

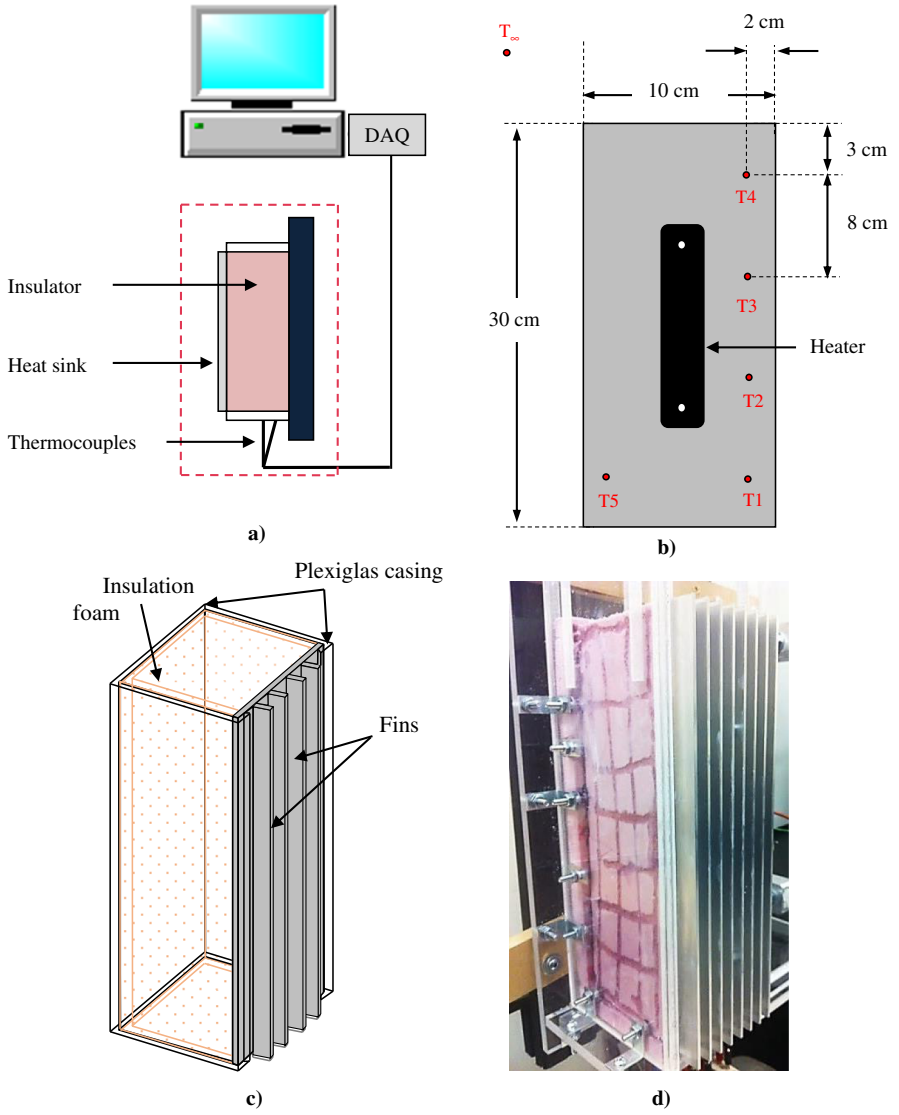

Fig. 4 Representations of a) schematic of the testbed; b) samples dimensions, heater, and thermocouple positioning; c) testbed casing and insulation; and d) photograph of the testbed.

$$\frac{\delta \dot{Q}_{\text{Rad.}}}{\dot{Q}_{\text{Rad.}}} = \left[4\left(\frac{\delta T_w}{T_w}\right)^2 + 4\left(\frac{\delta T_\infty}{T_\infty}\right)^2 + \left(\frac{\delta l}{l}\right)^2 + \left(\frac{\delta H}{H}\right)^2 + \left(\frac{\delta t}{t}\right)^2\right]^{1/2} \tag{26}$$

$$\dot{Q}_{\text{N.C.}}[W] = P_{\text{input}} + \dot{Q}_R \tag{27}$$

$$Nu_s = \frac{hs}{k} = \frac{\dot{Q}_{\text{N.C.}}}{\Delta T}\frac{s}{k} \tag{28}$$

Substituting the values for $V, I, T_w, T_\infty, l, H$, and t, respectively, into Eqs. (25) and (26), the maximum uncertainty value for Nu_s is calculated to be 4%. The measured temperature uncertainty ΔT is 1° C, which is twice the accuracy of the thermocouples. The calculated uncertainties for Nu_s is reported as error bars in the experimental results.

Table 5 Dimensions of the finned plate samples[a]

Sample no.	s, mm	N	H, mm	l, mm
1	9.5	8	17	300
2	6.0	12	17	300
3	14.0	6	17	300
4	9.5	8	10	300
5	9.5	8	25	300

[a]Note that the base plate width is similar in all samples; $W = 101$ mm.

VI. Results and Discussions

Figure 5 shows the comparison between the numerical results and the present analytical solution [Eqs. (21) and (22)] for the velocity and temperature distributions at different cross sections along the channel in the x direction. As shown, at the entrance of the channel, because of a sudden jump in temperature and velocity in the y direction due to the effects of wall, the integral technique cannot precisely predict the temperature and velocity profiles. This is an expected shortcoming of the integral technique, and it happens because we use continuous functions (second order polynomials) for both temperature and velocity distributions over the entire domain and these profiles cannot completely conform to the sudden changes in the flow characteristics at the entrance region. However, the agreement between the numerical data and the analytical model improves further away from the entrance region. Neglecting the entrance of the channel, $x \geq 0.01(Ra_s/\varepsilon)$ [48], the maximum relative differences for the velocity and temperature distribution between the present solution and the numerical simulation are 9.8 and 3.5%, respectively.

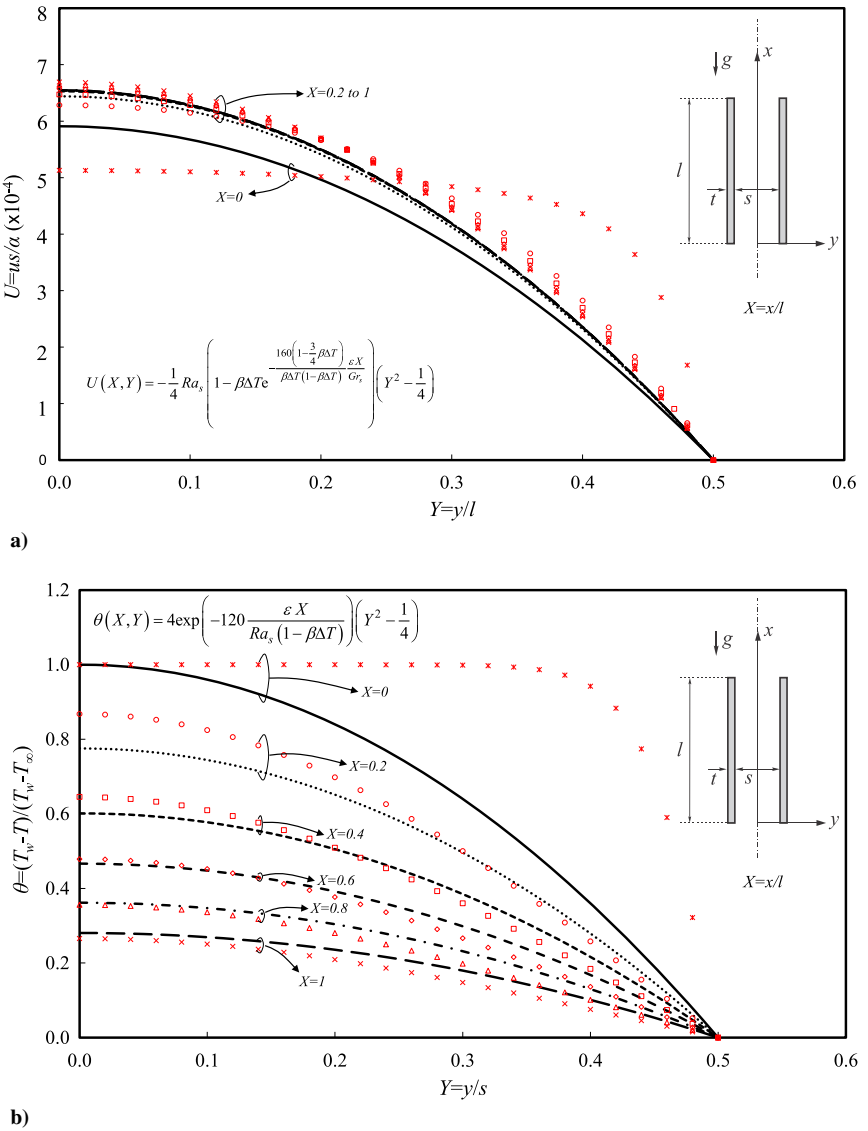

Fig. 5 Comparison between the present solutions (lines): a) velocity, and b) temperature distribution and numerical results (symbols) at various cross sections along the channel.

Local and average Nusselt numbers can be also calculated based on the temperature distribution obtained from the proposed analytical solution; Eq. (22). Equations (29) and (30) show the local and average Nusselt numbers for laminar natural convective heat transfer between two parallel plates as a function of the Rayleigh number; temperature difference; and the channel aspect ratio, $\varepsilon = l/s$:

$$Nu_s(X) = \frac{h(X)s}{k} = 4\,\exp\left(-180\frac{\varepsilon X}{Ra_s(1-\beta\Delta T)}\right) \tag{29}$$

$$Nu_s = \frac{hs}{k} = \frac{4}{14}\frac{Ra_s\left(1-\beta\Delta T\right)}{\varepsilon}\left[1-\exp\left(-180\frac{\varepsilon}{Ra_s(1-\beta\Delta T)}\right)\right] \tag{30}$$

Figure 6 shows a comparison between the proposed average Nusselt number, [Eq. (24)] and the semiempirical results from Elenbaas [17] and Bar-Cohen and Rohsenow [49] for $1000 \le Ra_s \le 4500$. As can be seen, for the mentioned Rayleigh numbers, there is a reasonable agreement between the present solution and the existing correlations in the literature with a maximum relative difference of 6%. The maximum relative different between the present semianalytical relationship for the Nusselt number and our experimental data is 1.6%. For higher Rayleigh numbers ($Ra_s > 4500$), as shown by Vorayos [48], the flow regime is similar to forced convection. In spite of being initiated by different mechanisms, the physics of the flow in the fully developed region is independent of how the flow is driven. Although, in the case of natural convection, the flow is buoyancy driven, due to the chimney effect, its behavior becomes similar to laminar forced convection [48].

VII. Conclusions

A new analytical solution for steady-state natural convection from isothermal parallel plates was presented. New, compact semi-analytical relationships were developed for velocity and temperature distributions for the buoyancy-driven channel flow. An integral method was used in combination with a power law assumption for the present analytical solution. An independent numerical simulation was performed using the commercially available software ANSYS FLUENT for validation purposes. A custom-made testbed was built, and five different aluminum heat sinks were prepare and tested to validate the numerical and semianalytical results. The proposed local temperature and velocity profile were compared with the numerical simulations, and good agreement was observed. For the first time, a semianalytical, compact and accurate model was proposed for the local and average Nusselt numbers in natural convection channel flow and successfully validated by experimental data.

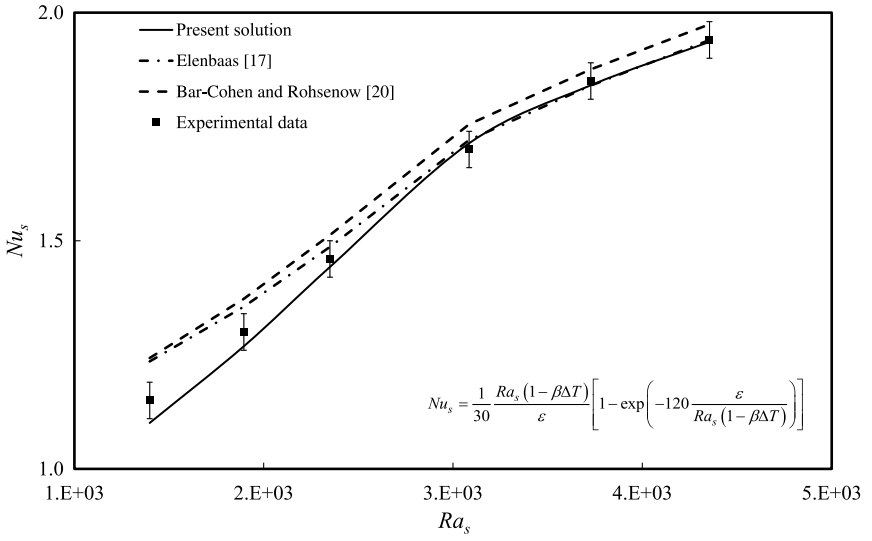

Fig. 6 Comparison between the present average Nusselt number, the existing semiempirical relations in the literature [17,49], and our experimental data.

Appendix: Integral Method for Natural Convection

In this appendix, the integral method for natural convection heat transfer is explained. The goal of this section is to clarify the methodology to obtain the governing equations from the control volumes shown in Table 2. The problem here is explained for a general case; however, extending the introduced equation here to the governing equations of Table 2 is straightforward.

Consider a boundary-layer flow driven by buoyancy forces originating from density variations in a fluid.

The integral conservation equations can be obtained by directly integrating the governing equations term by term across the control volume. Here, we start from first principles and perform mass, 10 momentum, and energy balances on the integral control volume shown in Fig. A1:

Conservation of mass (see Fig. A2):

$$\dot{m}_{\text{in}} - \dot{m}_{\text{out}} = \underbrace{\frac{\mathrm{d}}{\mathrm{d}t}(m_{CV})}_{=0} \quad \dot{m}_x = \int_0^\delta \rho u \,\mathrm{d}y$$

$$\dot{m}_{x+\mathrm{d}x} = \dot{m}_x + \frac{\partial}{\partial x}(\dot{m}_x)\,\mathrm{d}x \quad \therefore d\dot{m} = \frac{\mathrm{d}}{\mathrm{d}x}\left[\int_0^\delta \rho u \,\mathrm{d}y\right]\mathrm{d}x$$

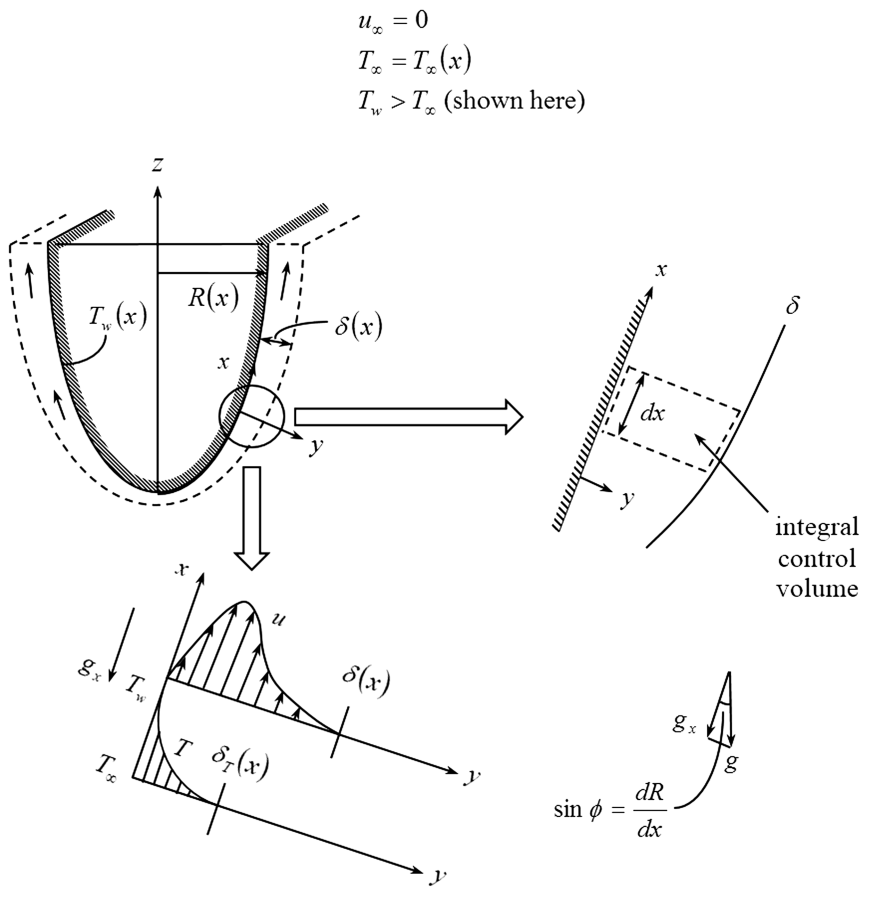

Fig. A1 Integral method for free convection.

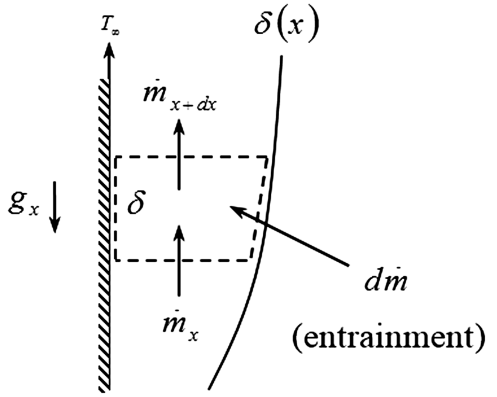

Fig. A2 Conservation of mass in control volume.

Conservation of x momentum (see Fig. A3):

$$\sum F_x + \dot{M}_{x,\text{in}} - \dot{M}_{x,\text{out}} = \underbrace{\frac{\mathrm{d}}{\mathrm{d}t}(M_{x,CV})}_{=0}$$

$$\therefore \int_0^\delta p_x \,\mathrm{d}y - \int_0^\delta p_{x+\mathrm{d}x}\,\mathrm{d}y = \int_0^\delta \rho_\infty g_x \,\mathrm{d}x\,\mathrm{d}y = \text{buoyancy force}$$

Thus, the x-momentum balance becomes

$$(-\tau_w \,\mathrm{d}x) + \int_0^\delta \rho_\infty g_x \,\mathrm{d}x\,\mathrm{d}y - \int_0^\delta \rho g_x \,\mathrm{d}x\,\mathrm{d}y + \dot{M}_x - \dot{M}_x - \frac{\partial}{\partial x}\underbrace{(\dot{M}_x)}_{=\int_0^\delta \rho u^2\,\mathrm{d}y}\mathrm{d}x = 0$$

Using $\rho_\infty - \rho = \rho\beta(T - T_\infty)$, we obtain

$$\frac{\mathrm{d}}{\mathrm{d}x}\left[\int_0^\delta u^2\,\mathrm{d}y\right] = \beta g_x \int_0^{\delta_T}(T - T_\infty)\,\mathrm{d}y - \frac{\tau_w}{\rho}$$

where the integration limits have been set, keeping in mind that $u = 0$ for $y > \delta$ and $T = T_\infty$ for $y > \delta_T$, and the shear stress at the wall can be defined as

$$\tau_w = -\mu\left.\frac{\partial u}{\partial y}\right|_{y=0}$$

Conservation of energy:

$$\dot{E}_{\text{in}} - \dot{E}_{\text{out}} = \underbrace{\frac{\mathrm{d}}{\mathrm{d}t}(E_{CV})}_{=0}$$

The dominant terms relevant to the energy balance are shown in Fig. A4. Consistent with the usual boundary-layer approximations, heat conduction in the x direction is neglected:

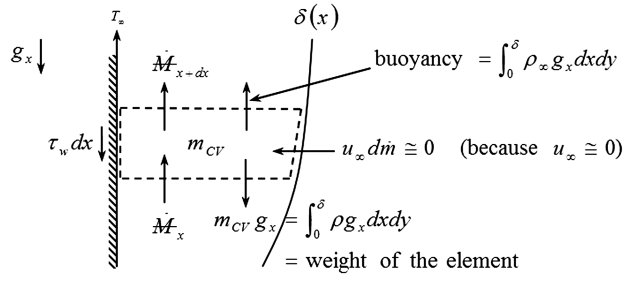

Fig. A3 Conservation of momentum in a control volume. Note that τ_w is per unit dept in the z direction.

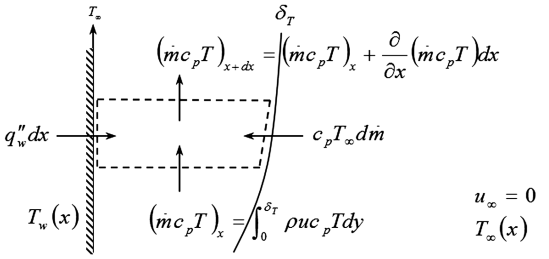

Fig. A4 Conservation of energy in control volume. Note that q''_w is per unit dept in the z direction.

$$q''_w\,\mathrm{d}x + c_pT_\infty\frac{\mathrm{d}}{\mathrm{d}x}\left[\int_0^\delta \rho u\,\mathrm{d}y\right]\mathrm{d}x - \frac{\mathrm{d}}{\mathrm{d}x}\left[\int_0^{\delta_T}\rho u c_p T\,\mathrm{d}y\right]\mathrm{d}x = 0$$

which can be rearranged to

$$\frac{\mathrm{d}}{\mathrm{d}x}\int_0^{\min(\delta,\delta_T)} u(T - T_\infty)\mathrm{d}y + \left(\frac{\mathrm{d}T_\infty}{\mathrm{d}x}\right)\int_0^\delta u\ \mathrm{d}y = \frac{q''_w}{\rho c_p}$$

where the heat flux at the wall can be defined as

$$q''_w = -k\left.\frac{\partial T}{\partial y}\right|_{y=0}$$

References

[1] Gurrum, S., and Suman, S., "Thermal Issues in Next-Generation Integrated Circuits," *IEEE Transactions on Device and Materials Reliability*, Vol. 4, No. 4, 2004, pp. 709–714. doi:10.1109/TDMR.2004.840160

[2] McGlen, R. J., Jachuck, R., and Lin, S., "Integrated Thermal Management Techniques for High Power Electronic Devices," *Applied Thermal Engineering*, Vol. 24, Nos. 8–9, June 2004, pp. 1143–1156. doi:10.1016/j.applthermaleng.2003.12.029

[3] Tawk, M., Avenas, Y., Kedous-Lebouc, A., and Petit, M., "Numerical and Experimental Investigations of the Thermal Management of Power Electronics With Liquid Metal Mini-Channel Coolers," *IEEE Transactions on Industry Applications*, Vol. 49, No. 3, May 2013, pp. 1421–1429. doi:10.1109/TIA.2013.2252132

[4] Wankhede, M., Khaire, V., and Goswami, A., "Evaluation of Cooling Solutions for Outdoor Electronics," *13th International Conference on Thermal Investigation of ICs and Systems*, EDA Publ., Budapest, 2007, pp. 1–6.

[5] Jahkonen, J., Puolakka, M., and Halonen, L., "Thermal Management of Outdoor LED Lighting Systems and Streetlights Variation of Ambient Cooling Conditions," *Leukos*, Vol. 9, No. 3, 2013, pp. 155–176. doi:10.1582/LEUKOS.2013.09.03.001

[6] Christensen, A., Ha, M., and Graham, S., "Thermal Management Methods for Compact High Power LED Arrays," *7th International Conference on Solid State Lighting*, edited by Ferguson, I. T., Narendran, N., Taguchi, T., and Ashdown, I. E., SPIE, Bellingham, WA, 2007, Paper 66690Z.

[7] "The Market for Thermal Management Technologies," BCCResearch Rept. SMC024J, Wellesley, MA, 2014.

[8] "Information and Communication Technology Portfolio: Improving Energy Efficiency and Productivity in America's Telecommunication Systems and Data Centers," U.S. Dept. of Energy Brochure, 2012.

[9] Roy, S. N., "Energy Logic: A Road Map to Reducing Energy Consumption in Telecom Munications Networks," *2008 IEEE 30th International Telecommunications Energy Conference*, IEEE, Piscataway, NJ, Sept. 2008, pp. 1–9.

[10] Lange, C., Kosiankowski, D., Weidmann, R., and Gladisch, A., "Energy Consumption of Telecommunication Networks and Related Improvement Options," *IEEE Journal of Selected Topics in Quantum Electronics*, Vol. 17, No. 2, March 2011, pp. 285–295. doi:10.1109/JSTQE.2010.2053522

[11] Lange, C., Kosiankowski, D., Gerlach, C., Westphal, F., and Gladisch, A., "Energy Consumption of Telecommunication Networks," *35th European Conference on Optical Communication (ECOC-09)*, IEEE, Piscataway, NJ, 2009, pp. 1–2.

[12] Kilper, D. C., Member, S., Atkinson, G., Korotky, S. K., Goyal, S., Vetter, P., Suvakovic, D., and Blume, O., "Power Trends in Communication Networks," *IEEE Journal of Selected Topics in Quantum Electronics*, Vol. 17, No. 2, 2011, pp. 275–284. doi:10.1109/JSTQE.2010.2074187

[13] Lubritto, C., and Petraglia, A., "Telecommunication Power Systems: Energy Saving, Renewable Sources and Environmental Monitoring," *IEEE Electrical Power and Energy Conference (EPEC)*, IEEE, Piscataway, NJ, 2008, pp. 1–4.

[14] Hernon, D., Silvestre-Castillo, P., and Hayden, P., "Significantly Extending the Operational Range of Free Cooling in Radio Base Station Indoor Shelters," *IEEE 33rd International Telecommunications Energy Conference (INTELEC)*, IEEE, Piscataway, NJ, 2011, pp. 1–7.

[15] Yousefi, T., and Ashjaee, M., "Experimental Study of Natural Convection Heat Transfer from Vertical Array of Isothermal Horizontal Elliptic Cylinders," *Experimental Thermal and Fluid Science*, Vol. 32, No. 1, Oct. 2007, pp. 240–248. doi:10.1016/j.expthermflusci.2007.04.001

[16] Suryawanshi, S., and Sane, N., "Natural Convection Heat Transfer from Horizontal Rectangular Inverted Notched Fin Arrays," *Journal of Heat Transfer*, Vol. 131, No. 8, 2009, pp. 797–805. doi:10.1115/1.3109993

[17] Elenbaas, W., "Heat Dissipation of Parallel Plates by Free Convection," *Physica*, Vol. 9, No. 1, Jan. 1942, pp. 1–28. doi:10.1016/S0031-8914(42)90053-3

[18] Churchill, S. W., "A Comprehensive Correlation Equation for Buoyancy Induced Flow in Channels," *Letters in Heat and Mass Transfer*, Vol. 4, No. 3, 1977, pp. 193–199.

[19] Churchill, S. W., and Chu, H., "Correlating Equations for Laminar and Turbulent Free Convection from a Vertical Plate," *International Journal of Heat and Mass Transfer*, Vol. 18, No. 11, 1975, pp. 1323–1329. doi:10.1016/0017-9310(75)90243-4

[20] Bar-Cohen, A., and Rohsenow, W. M., "Thermally Optimum Spacing of Vertical Natural Convection Cooled Parallel Plates," *Transactions of the American Society of Mechanical Engineers*, Vol. 106, No. 1, 1984, pp. 116–123. doi:10.1115/1.3246622

[21] Bodoia, J. R., and Osterle, J. F., "The Development of Free Convection Between Heated Vertical Plates," *Journal of Heat Transfer*, Vol. 84, No. 1, 1962, pp. 40–43. doi:10.1115/1.3684288

[22] Ofi, O., and Hetherington, H. J., "Application of the Finite Element Method to Natural Convection Heat Transfer from the Open Vertical Channel," *International Journal of Heat and Mass Transfer*, Vol. 20, No. 11, Nov. 1977, pp. 1195–1204. doi:10.1016/0017-9310(77)90128-4

[23] Culham, J. R., Yovanovich, M. M., and Lee, S., "Thermal Modeling of Isothermal Cuboids and Rectangular Heat Sinks Cooled by Natural Convection," *IEEE Transactions on Components, Packaging, and Manufacturing Technology: Part A*, Vol. 18, No. 3, 1995, pp. 559–566. doi:10.1109/95.465153

[24] Sparrow, E. M., and Acharya, S., "A Natural Convection Fin with a Solution-Determined Nonmonotonically Varying Heat Transfer Coefficient," *Journal of Heat Transfer*, Vol. 103, No. 2, 1981, pp. 218–226. doi:10.1115/1.3244444

[25] Starner, K. E., and McManus, H. N., "An Experimental Investigation of Free-Convection Heat Transfer from Rectangular-Fin Arrays," *Journal of Heat Transfer*, Vol. 85, No. 3, 1963, pp. 273–275. doi:10.1115/1.3686097

[26] Welling, J. R., and Wooldridge, C. B., "Free Convection Heat Transfer Coefficients from Rectangular Vertical Fins," *Journal of Heat Transfer*, Vol. 87, No. 4, 1965, pp. 439–444. doi:10.1115/1.3689135

[27] Edwards, J., and Chaddock, J., "An Experimental Investigation of the Radiation and Free Convection Heat Transfer from a Cylindrical Disk Extended Surface," *ASHRAE Transactions*, Vol. 69, No. 1, 1963, pp. 313–322.

[28] Chaddock, J., "Free Convection Heat Transfer from Vertical Rectangular Fin Arrays," *ASHRAE Journal*, Vol. 12, Aug. 1970, pp. 53–60.

[29] Aihara, T., "Natural Convection Heat Transfer from Vertical Rectangular Fin Arrays: Part 3, Heat Transfer from Fin Flats," *Transactions of the Japan Society of Mechanical Engineers*, Vol. 13, No. 64, 1970, pp. 1192–1200. doi:10.1299/jsme1958.13.1192

[30] Aihara, T., "Natural Convection Heat Transfer from Vertical Rectangular Fin Arrays: Part 2, Heat Transfer from Fin Edges," *Transactions of the Japan Society of Mechanical Engineers*, Vol. 36, No. 282, 1970, pp. 239–247. doi:10.1299/kikai1938.36.239

[31] Aihara, T., "Natural Convection Heat Transfer from Vertical Rectangular Fin Arrays: Part 1, Heat Transfer from Base Plates," *Transactions of the Japan Society of Mechanical Engineers*, Vol. 34, No. 261, 1968, pp. 915–926. doi:10.1299/kikai1938.34.915

[32] Aihara, T., "Natural Convection Heat Transfer from Vertical Rectangular-Fin Arrays : Part 4, Heat-Transfer Characteristics of Nonisothermal-Fin Arrays," *Transactions of the Japan Society of Mechanical Engineers*, Vol. 36, No. 292, 1970, pp. 2077–2086. doi:10.1299/kikai1938.36.2077

[33] Leung, C. W., and Probert, S. D., "Heat Exchanger: Optimal Separation for Vertical Ractangualr Fins Proturding from Vertical Rectangular Base," *Applied Energy*, Vol. 19, No. 2, 1985, pp. 77–85. doi:10.1016/0306-2619(85)90063-7

[34] Leung, C. W., Probert, S. D., and Shilston, M. J., "Heat Exchanger Design: Optimal Uniform Separation Between Rectangular Fins Protruding from a Vertical Rectangular Base," *Applied Energy*, Vol. 19, No. 4, Jan. 1985, pp. 287–299. doi:10.1016/0306-2619(85)90003-0

[35] Leung, C., Probert, S., and Shilston, M., "Heat Exchanger Design: Thermal Performances of Rectangular Fins Protruding from Vertical or Horizontal Rectangular Bases," *Applied Energy*, Vol. 20, No. 2, 1985, pp. 123–140. doi:10.1016/0306-2619(85)90029-7

[36] Leung, C., Probert, S., and Shilston, M., "Heat Transfer Performances of Vertical Rectangular Fins Protruding from Rectangular Bases: Effect of Fin Length," *Applied Energy*, Vol. 22, No. 4, 1986, pp. 313–318. doi:10.1016/0306-2619(86)90040-1

[37] Leung, C. W., and Probert, S. D., "Natural-Convective Heat Exchanger with Vertical Rectangular Fins and Base: Design Criteria," *Journal of Mechanical Engineering Science*, Vol. 201, Sept. 1987, pp. 365–372. doi:10.1243/PIME_PROC_1987_201_136_02

[38] Leung, C. W., and Probert, S. D., "Heat-Exchanger Performance: Effect of Orientation," *Applied Energy*, Vol. 33, No. 4, Jan. 1989, pp. 235–252. doi:10.1016/0306-2619(89)90057-3

[39] Leung, C. W., and Probert, S. D., "Thermal Effectiveness of Short-Protrusion Rectangular Heat Exchanger Fins," *Journal of Applied Energy*, Vol. 34, No. 1, 1989, pp. 1–8. doi:10.1016/0306-2619(89)90050-0

[40] Van de Pol, D., and Tierney, J., "Free Convection Heat Transfer from Vertical Fin-Arrays," *IEEE Transactions on Parts, Hybrids, and Packaging*, Vol. 10, No. 4, 1974, pp. 267–271. doi:10.1109/TPHP.1974.1134861

[41] Anandan, S., and Ramalingam, V., "Thermal Management of Electronics: A Review of Literature," *Thermal Science*, Vol. 12, No. 2, 2008, pp. 5–26. doi:10.2298/TSCI0802005A

[42] Bejan, A., *Convection Heat Transfer*, Wiley, New York, 2004, pp. 178–202.

[43] Sparrow, E. M., and Gregg, J. L., "Similar Solutions for Natural Convection from a Non Isothermal Vertical Plate," *Journal of Heat Transfer*, Vol. 80, No. 1, 1958, pp. 379–386.

[44] Sparrow, E. M., and Gregg, J. L., "Laminar Free Convection Heat Transfer from the Outer Surface of a Vertical Circular Cylinder," *Transactions of the American Society of Mechanical Engineers*, Vol. 78, No. 1, 1956, pp. 1823–1829.

[45] Gebhart, B., Pera, L., and Schorr, A., "Steady Laminar Natural Convection Plumes Above a Horizontal Line Heat Source," *International Journal of Heat and Mass Transfer*, Vol. 13, No. 1, Jan. 1970, pp. 161–171. doi:10.1016/0017-9310(70)90032-3

[46] Jaluria, Y., and Gebhart, B., "Buoyancy-Induced Flow Arising from a Line Thermal Source on an Adiabatic Vertical Surface," *International Journal of Heat and Mass Transfer*, Vol. 20, No. 2, Feb. 1977, pp. 153–157. doi:10.1016/0017-9310(77)90007-2

[47] Holman, J. P., *Experimental Methods for Engineers*, McGraw–Hill, New York, 2001, pp. 48–141.

[48] Vorayos, N., "Laminar Natural Convection Within Long Vertical Uniformly Heated Parallel-Plate Channels and Circular Tubes," Ph.D. Thesis, Oregon State Univ., Corvallis, OR, 2000.

[49] Bar-Cohen, A., and Rohsenow, W. M., "Thermally Optimum Spacing of Vertical, Natural Convection Cooled, Parallel Plates," *Journal of Heat Transfer*, Vol. 106, No. 1, 1984, pp. 116–123. doi:10.1115/1.3246622